Solution Treatment Effects on Microstructure and Mechanical Properties of Al-(1 to 13 pct)Si-Mg Cast Alloys

DIANA A. LADOS, DIRAN APELIAN, and LIBO WANG

The effects of solution treatment time and Si content and morphology on microstructures and mechanical properties of heat-treated Al-Si-Mg cast alloys were investigated systematically. Five alloys, with Si levels ranging from 1 to 13 pct, were tested in as-cast, T4, and T61 conditions. The eutectic Si was both unmodified and Sr-modified. Results show that the microstructures are affected significantly by alloy composition, eutectic Si morphology, and solution treatment time. Si content has significant effects on ultimate tensile strength (UTS), yield strength (YS), and elongation as well as a strong influence on solution treatment response. In T61 treatment with different solutionizing times, UTS and YS reach their maximum values in ~1 hour of solutionizing followed by a decrease, then a slight increase, and finally, a plateau close to the maximum level. Elongation of alloys with a high Si content, 7 pct and 13 pct, increases rapidly at solutionizing times of 1 to 2 hours then varies in a wide range, showing improvements in the 4 to 10 hours range. The data indicate that a solution treatment time of ~1 hour is sufficient to achieve maximum strength. The changes in mechanical properties were correlated to changes in microstructure evolution—Mg-Si precipitation, Si particle fragmentation, and microstructure homogenization. Empirical models uniquely relating Si content to UTS and YS are given for T61 heat-treated alloys.

I. INTRODUCTION

CAST Al-Si-Mg alloys are used in a wide variety of tempers. For noncritical applications, castings may be put into service in the as-cast condition (F-temper) or with only a low-temperature T5 stabilization treatment. Most critical castings, however, generally are used in T6 or T7 heat-treated conditions. These treatments consist of solution treatment, quenching, and natural and/or artificial aging. The improvement in tensile properties through heat treatment mainly is attributed to the formation of the nonequilibrium Mg_2Si precipitates within the Al matrix.[1,2] In regard to Mg_2Si formation, solution treatment and quenching can be considered a preparatory step for aging. Extensive research has been conducted on solution treatment, and it has been reported that the solution treatment time currently used and recommended in standards such as 811 K (538 °C) for 10 hours for 356 alloys is unnecessarily long. For example, studying the Mg and Si concentrations within Al dendrites for 356 alloys in as-cast condition and after different solution treatment times, Closset et al.[3] found that the dissolution of Mg_2Si particles and homogenization was essentially complete within 0.5 hours at 823 K (550 °C). Even though many investigators have shown that the solution treatment time can be shortened significantly, specifications remain unchanged.

Si is the major alloying element in heat-treatable cast Al-Si-Mg alloys, and Si particles represent a large volume fraction of the alloy's microstructure. Much work has been done relating the size and morphology evolution of Si particles and its effects on properties.[4,5] However, what is missing in the literature is a mechanistic understanding of the effects of Si content at each stage of the heat-treatment process. Accordingly, a systematic study of the role of Si on the heat-treatment response of Al-Si-Mg cast alloys was conducted in two phases. The first phase focuses on the role of Si on solution treatment, and the findings are presented in this article. The second phase investigates the role of Si on artificial aging that will be presented in a subsequent article.

II. BACKGROUND

It has been reported that the evolution of the eutectic Si undergoes the following successive stages: (1) fragmentation, (2) spheroidization, and (3) coarsening.[4] However, other studies question the existence of these distinct stages or point to different time spans for each stage. For example, Li et al.[5] showed that for A356 alloys, Sr modification has a profound influence on spheroidization kinetics. In modified alloys, a high degree of spheroidization was observed after 12 hours of solution treatment, whereas in unmodified alloys, even after 12 hours, coarse Si plates were still visible.

DIANA A. LADOS, Assistant Professor of ME and Director, is with the Integrative Materials Design Center, Worcester Polytechnic Institute, Worcester, MA 01609. Contact e-mail: lados@wpi.edu. DIRAN APELIAN, Howmet Professor of ME and Director, and LIBO WANG, Research Professor, are with the Metal Processing Institute, Worcester Polytechnic Institute.

Parker et al.[6] have shown that in a Sr-modified Al-7 pctSi-0.45 pctMg alloy, spheroidization occurred at short times (10 minutes) of solution treatment. Pan et al.[7] showed that no fragmentation and spheroidization stages were present. In this study, the optical microscopy revealed that in Sr-modified A357 alloys, the relatively large, as-cast Si particles in a 10-mm-thick sand casting plate were fragmented into small pieces during the first 4 hours. Then, the fragmented Si particles were spheroidized to a more rounded shape in the 6-to-12-hour range, and subsequently, the spheroidized particles grew larger. However, when observed under SEM, these apparently separate particles in fact still were interconnected. It also has been shown that the large Si particles formed in thicker castings were not fragmented even after 22 hours; the sharp-edged as-cast Si particles gradually became rounder and stubbier, forming necking, but still they remained interconnected.

Similar phenomena to those observed by Pan et al.[7] were reported by Pedersen and Arnberg,[8] who discussed the differences between unmodified and modified alloys. In the unmodified alloys, the edges of the Si plates first are rounded. Next, the finer plates begin to fragment, whereas the coarser plates start to form "bays" stretching from the periphery into the plates. With the increase in solutionizing time, the bays become deep, and rod-like areas form. In the modified alloys, fine rods build up the structure even before heat treatment. The well-modified structure spheroidizes more rapidly than the coarse plates in the unmodified alloys, and some coarsening takes place with time. Meyers proposed a model for the solution treatment of A357 alloys[9]; he reported that a process closely resembling coarsening occurred during solution treatment and that reversed growth and homogenization played a minor role. Meyers reported that the radii of Si particles increased with the cubic root of solution treatment time; the density of Si particles decreased while their size increased with increasing time, and coarsening was temperature sensitive.[8] Earlier work at Worcester Polytechnic Institute (WPI) showed that extremely high coarsening occurred at temperatures greater than 833 K (560 °C) for A356.2 alloys.[10]

In regard to the effect of Si on mechanical properties of heat-treated castings, Pan et al.[7] showed that both ultimate tensile strength (UTS) and yield strength (YS) of A357 alloys first increased and then decreased with an increase in solution treatment time. Maximum values were reached at times corresponding to the Si morphology (in two-dimensional [2D] images) attained at the late stage of spheroidization or early stage of coarsening. This corresponded to 6 to 10 hours for tensile test bars treated at 803 K (530 °C) to 811 K (538 °C). In all cases, elongation increased progressively with increasing solution time. In the study of 354 and 353 alloys, Li observed that mechanical properties were related closely to the average aspect ratio of the Si particles.[11] With the rapid decrease of the average aspect ratio at the beginning of the solution treatment, the tensile and yield strengths of both alloys increased significantly. After 1 hour, with the slower change of the aspect ratio, the UTS and YS remained almost the same up to 24 hours,

whereas, the elongation was improving continuously until ~12 hours. Meyers' work on the A357 alloys reported that all mechanical properties showed an improving trend with the increase in solution time and the resulting Si particle coarsening.[12] The data showed that the best mechanical properties were obtained in about 10 to 15 hours of solution treatment. Pedersen and Arnberg[8] found that for Al-7Si-Mg alloys the maximum strength was obtained at ~1 hour of solution treatment and prolonged solution treatments did not lead to any additional increase in strength. In general, ductility decreased at the beginning of the solution treatment, reached the minimum at about 1 hour, and then increased noticeably for solution treatment times in the 1- to -4-hour range. The variation in mechanical properties was attributed to the combined effects of the following microstructural factors: the microstresses resulting from the formation of metastable β'-Mg_2Si precipitates and the changes in Si particle morphology.

As for the effect of the Si content, the precipitation hardening of Mg_2Si occurred in less time for alloys containing excess Si.[13] The "excess Si" refers to any Si dissolved in the solid solution exceeding the stoichiometric amount necessary to form Mg_2Si precipitates. For example, 0.4 pct Mg in an alloy needs about 0.23 pct Si to form Mg_2Si precipitates. Thus, in alloys containing 0.4 pct Mg, when the Si content is greater than 0.23 pct, the alloy will contain excess Si (the solubility of Si in Al is approximately 1.4 pct at 811 K [538 °C]). Lynch et al.[14] pointed out that during the first stage of precipitation, the composition of the precipitates in the Al-Si-Mg system alloys could not be described as Mg_2Si, but rather as $Mg_{0.44}Si$. To form $Mg_{0.44}Si$, for alloys with 0.4 pct Mg, it needs ~1.05 pct Si. This implies that Si is one of the factors controlling the decomposition of the supersaturated solution. When the concentration of Si in the supersaturated solution is high, the time required for the formation and growth of nuclei is short because of the reduced diffusion distances.

Unlike the effect of Si morphology, the literature is devoid of any knowledge of the effect of Si content on heat treatment response. Even though information in this sense can be deduced secondarily from some studies, it is limited and inconsistent. For example, in studying the effects of solution treatment and quenching rate on the mechanical properties and microstructures of Al-Si-Mg alloys (Si levels of 7 and 11 pct), Pedersen and Arnberg[8] found that the ductility was related strongly to the amount of Si and the fineness of the eutectic Si particles. However, the strength of the alloys was nearly independent of the Si level. Kashyap et al.[15] reported that the effect of Si content on strength was related to the Mg content. At a low Mg level (0.1 pct), the increase of Si from 7 to 11 pct increased the UTS, but when the Mg level was increased to 0.3 pct, only minor changes in UTS were observed. Langsrud et al.[16] developed a semiempirical model and a software "AlProp" in which the tensile properties of AlMgSi(Fe)(Sr) alloys with Si can be predicted. YS is influenced by the eutectic and by the preeutectic structures. This implies that the strength is related to the Si content because the Si content determines the eutectic fraction in the structure.

The model shows that the total elongation decreases with increasing Si. However, Langsrud's model treats the Si content independently of the solution treatment. In studying the solution treatment of the alloys 354 (9.0 pct Si, 0.5 pct Mg) and 355 (5.0 pct Si, 0.5 pct Mg), Li[11] showed that at a temperature of 800 K (527 °C) both alloys reached their maximum strengths around 10 to 12 hours, and the alloy 354 showed higher strength and a slightly lower elongation. The major difference between the two alloys is the Si content, 9 pct in 354 and 5 pct in 355, which could imply that higher Si resulted in higher strength and lower elongation. However, the authors only emphasized the effects of the Si morphological variations and ignored the obvious difference in Si content.

III. EXPERIMENTAL PROCEDURE

A. Alloys

The focus of this study is Al-Si-Mg cast alloys with a Mg content fixed at 0.45 pct. This Mg level is used commonly in A356 and 357 Al-Si-Mg cast alloys, which have combined Mg ranges from 0.17 to 0.7 pct. Also, based on the literature, a Mg content level of 0.45 pct ensures that sufficient Mg_2Si precipitates can be produced for alloy strengthening during heat treatment. Three levels of Si—1, 7, and 13 pct—were selected for this study, which resulted in different amounts of Si eutectic structure. In Al-Si-0.45 pct Mg alloys, 1 pct Si does not form any eutectic Si structure, and the level of Si is sufficient for the 0.45 pct Mg to form Mg_2Si precipitates. The alloys with 13 pct Si produce the maximum amount of eutectic structure without forming primary Si particles, and the 7 pct Si alloys represent an intermediary condition akin to A356 alloys.

To create a distinct Si morphology for the unmodified and modified Si eutectic structures while maintaining the same grain size in all alloys (~300 μm), the amounts of Sr and Ti were controlled carefully using Al-10 pct Sr and Al-5 pct Ti-1 pct B master alloys (Table I). The remaining elements were kept at sufficiently low levels, <0.002 pct, to not introduce measurable effects on the mechanical properties of the alloys. Special attention was paid to Fe; because of its detrimental effects on mechanical properties, the Fe level was kept below 0.02 pct.

The five alloys produced and studied are Al-1 pct Si-0.45 pct Mg (alloy 1), Al-7 pct Si-0.45 pct Mg-unmodified (alloy 2), Al-7 pct Si-0.45 pct Mg-modified (alloy 3), Al-13 pct Si-0.45 pct Mg-unmodified (alloy 4),

and Al-13 pct Si-0.45 pct Mg-modified (alloy 5). The compositions of the alloys are shown in Table I. All casting conditions were designed appropriately and implemented arduously to result in samples with constant secondary dendrite arm spacing, SDAS~25 μm.

B. Alloys and Test Specimens Preparation

The alloys were prepared in an induction furnace using a SiC crucible with the following charging materials: high-purity Al ingots, high-purity Si, Al-25 pct Mg master alloy, Al-10 pct Sr modifier, and 5 pct Ti-1 pct B grain refiner. The melts all were degassed using a rotary impeller degasser and argon gas to minimize the hydrogen level; all cast alloys had a hydrogen content lower than 0.1 cc/100 g.

The pouring temperatures were set such that all alloys had the same superheat of ~125 K (°C). For this reason, the cooling curves were evaluated a priori in a small sand cup to determine the liquidus temperatures; the results are shown in Figure 1. Accordingly, the pouring temperatures were set at 983 K (710 °C) for alloys 4 and 5 (13 pct Si), 1018 K (745 °C) for alloys 2 and 3 (7 pct Si), and 1053 K (780 °C) for alloy 1 (1 pct Si), representing a superheat of ~125 K (°C).

Standard tensile test specimens with 12.7 mm (0.5 in) in diameter (ASTM Standard B557) were cast in a vertical open-book die (Stahl mold) made of cast iron. The mold preheat temperature was approximately 723 K (450 °C) 728 K (455 °C). For each alloy, 100 to 120 test bars were produced from four heats. For each heat, the alloy chemistry sample was taken in the middle of the pour. The chemistries reported in Table I represent the calculated averages and the ± values represent
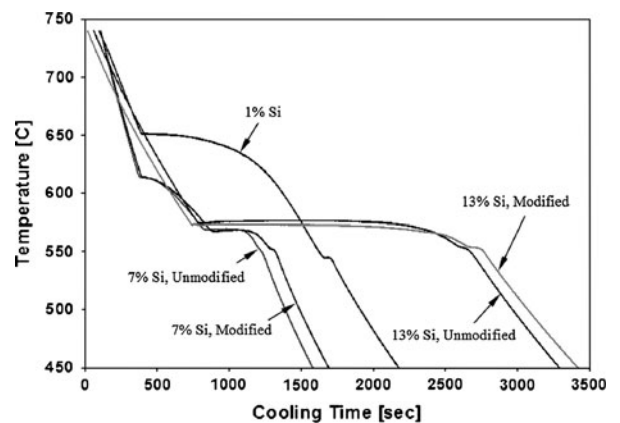

Fig. 1—Cooling curves of the five alloys evaluated.

Table I. Chemical Compositions of the Studied Alloys

Alloy	Si	Mg	Ti	Sr	Fe	Others
Alloy 1	1.0 ± 0.1	0.45 ± 0.02	0.0070 ± 0.0005		<0.02	<0.002
Alloy 2	7.0 ± 0.1	0.45 ± 0.02	0.04 ± 0.005		<0.02	<0.002
Alloy 3	7.0 ± 0.1	0.45 ± 0.02	0.03 ± 0.005	0.019 ± 0.002	<0.02	<0.002
Alloy 4	13.0 ± 0.1	0.45 ± 0.02	0.28 ± 0.02		<0.02	<0.002
Alloy 5	13.0 ± 0.1	0.45 ± 0.02	0.22 ± 0.02	0.025 ± 0.002	<0.02	<0.002

the maximum variations among different heats and measurements.

C. *Heat Treatment*

The solution treatment temperature was 811 K (538 °C), a value recommended in most references and widely used in production for A356 type alloys. Starting from room temperature, the ramp-up time to 805 K (532 °C) was ~1.5 hours, and an additional 10 to 20 minutes were needed to stabilize the temperature at 811 K (538 °C). Once stabilized, the temperature variation was ±1.5 K (°C), and the solution treatment time commenced. The experimental solution treatment times were 0.5, 1, 1.5, 2, 4, 6, 8, and 10 hours. After quenching, the specimens were left in air at room temperature (natural aging) for 12 hours. For each alloy, from each solution treatment time group, five specimens then were aged artificially at 428 K (155 °C) for 12 hours, with the time selected based on aging experiments (the results of the aging studies will be presented in a subsequent article) to minimize the effect of aging parameters on the solution treatment study. The artificial aging was started 12 hours after the last group of solution-treated specimens (corresponding to the longest solution treating time of 10 hours) was quenched. For the artificial aging, the ramp-up time to 423 K (150 °C) was ~1 hour, and 10 to 20 more minutes were needed to stabilize the temperature at 428 K (155 °C). Once stabilized, the temperature variation was ±1.5 K (°C), and the aging time commenced.

D. *Tensile Testing and Microstructural Analysis*

Tensile tests were conducted at room temperature according to ASTM B557. The strain was measured using an axial extensometer with a gage length of 50 mm. The ramp rate was set at ~1 mm/min, and extensometer measurements were taken until the specimen was fractured. For each specimen, the UTS, YS, elongation (e pct), and modulus of elasticity (E) were derived. For each alloy, the following conditions/ samples were tested: five as-cast samples, five samples for each solution treatment time plus artificial aging (T61), and five samples that were only solution treated (T4) for 10 hours.

For metallographic analysis, the samples were sectioned from the reduced section of the test bar near the fracture surface. The samples for the 2D analysis were etched using a solution of 1 pct HF and 99 pct H_2O and observed through optical microscopy. A solution of 20 pct NaOH was used to deep etch the samples for three-dimensional (3D) observation via scanning electron microscopy (SEM). For grain structure, Barker reagent (950 ml H_2O and 50 ml HBF_4) and electro-etching with direct current voltage of 30 V were used, and the grain morphologies were observed under polarized light. Energy-dispersive X-ray spectroscopy was used to identify the different phases and their constituents. The microstructures and the phase morphology were analyzed quantitatively using image analysis.

IV. RESULTS

A. *Microstructure*

Figures 2 and 3 represent the microstructures of the alloys after solution treatment for different times. Figure 2 shows images observed via optical microscopy, whereas Figure 3 reveals the 3D structure of the phases observed via SEM on deep-etched surfaces. It can be noted that the morphology of the eutectic Si particles changes significantly with solution treatment time and that it also is affected by the original (as-cast) particle size and morphology.

The size and shape of the as-cast eutectic Si particles depend on the melt treatment used, such as level of modification. The as-cast unmodified Si particles are in the form of plates, as shown in Figure 3 for alloys 2 (7 pct Si) and 4 (13 pct Si). The as-cast Sr-modified eutectic Si has a 3D coral-like structure (Figure 3— alloys 3 and 5), which projects as small round spots on the as-polished 2D surfaces, (Figure 2—alloys 3 and 5). The microstructural images in Figure 3 show that during solution treatment the eutectic Si undergoes the following transformations: fragmentation, spheroidization, and growth. The dominant phenomenon at any given time depends on the treatment temperature and the size and morphology of the original particles. The effect of treatment temperature was studied by Shivkumar *et al.*[10] The study showed that higher temperatures accelerated the whole process. For example, a great difference was observed, even after 0.5 hours of solution treatment, when the solution temperature was increased from 538 °C (1000 °F) to 554 °C (1030 °F). The current study clearly shows the effect of the size and morphology of the original particles. Most fragmentation occurred in less than 0.5 hours for the modified alloys 3 and 5 (7 and 13 pct Si), whereas the fragmentation continued after 4 hours (even though the most significant transformations occurred within 1.5 hours) for the unmodified alloys 2 and 4 (7 and 13 pct Si) (Figure 3). In the modified alloys, the Si particles became rounder and started to grow in less than 0.5 hours, whereas in the unmodified alloys, no significant growth was observed even after 10 hours of solution treatment.

The variations of the Si particle size and shape factor (reflecting the particle roundness) for 7 pct Si alloys (alloy 2, unmodified; and alloy 3, Sr-modified) with solution treatment time are shown in Figures 4(a) and (b). All measurements were carried out using image analysis on 2D images. For both unmodified and modified alloys, the shape factors drop dramatically at the beginning (in the first 0.5 hours), after which the drop continues for the unmodified alloys at a slow rate, whereas almost no change is observed in the modified alloys. Although the shape factors of the unmodified alloys are always greater than those of the modified alloys, the difference reduces with an increasing solution treatment time. In regard to particle size, the data show that the size of the unmodified particles decreases at the beginning and starts to increase after approximately 0.5 hours, whereas the size of the modified particles increases continuously with a fast rate at the beginning
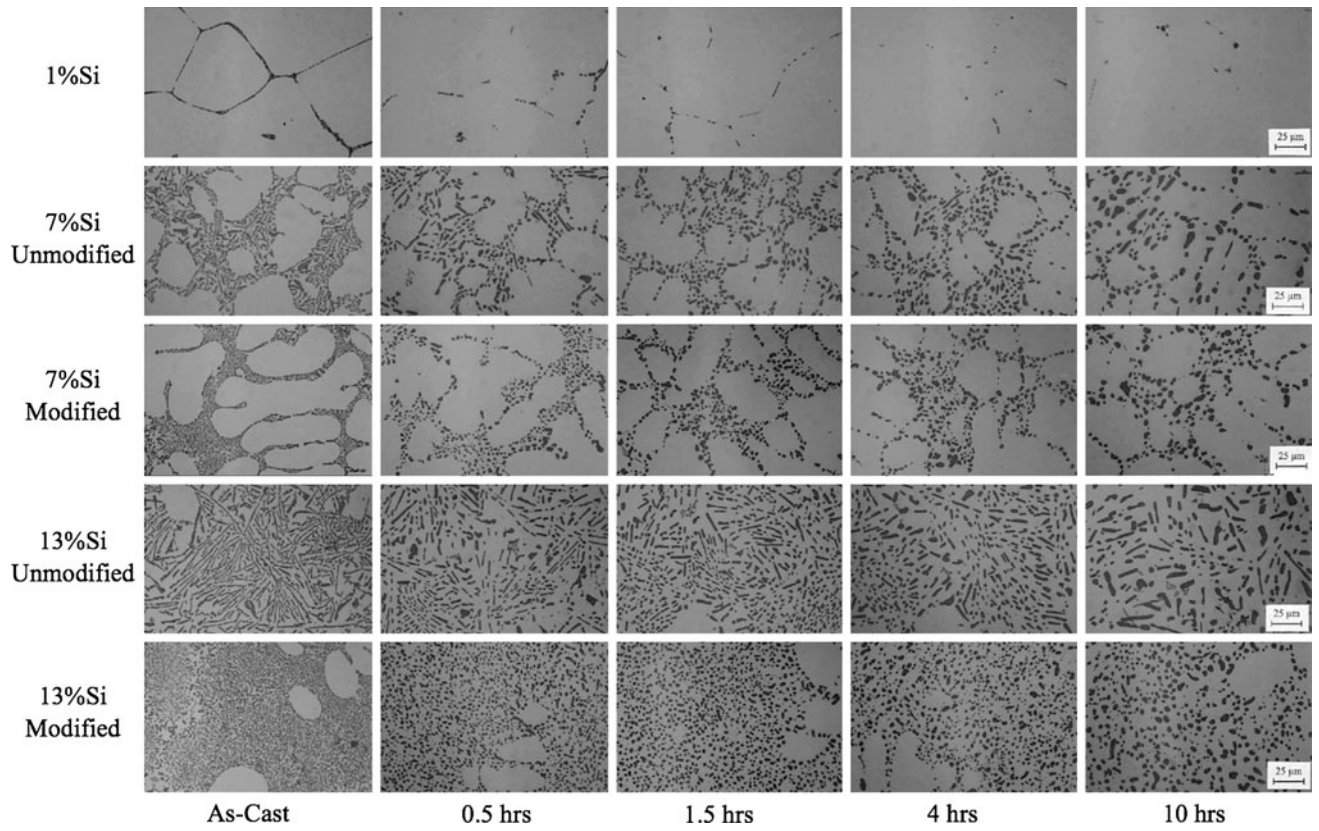
Fig. 2—Microstructures of the five studied alloys after various solution treatment times as observed under the optical microscope.
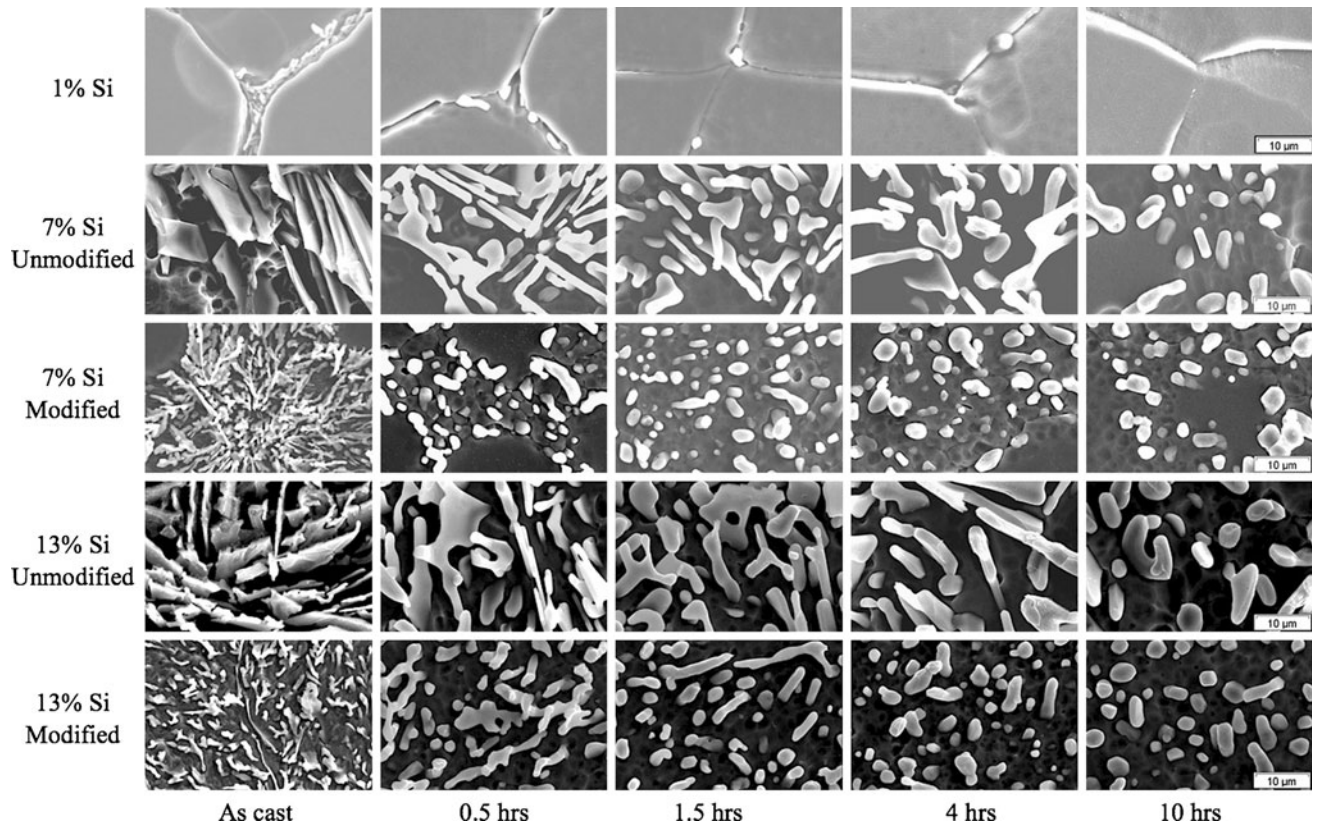

Fig. 3—Microstructures of the five studied alloys after various solution treatment times as observed under the SEM.
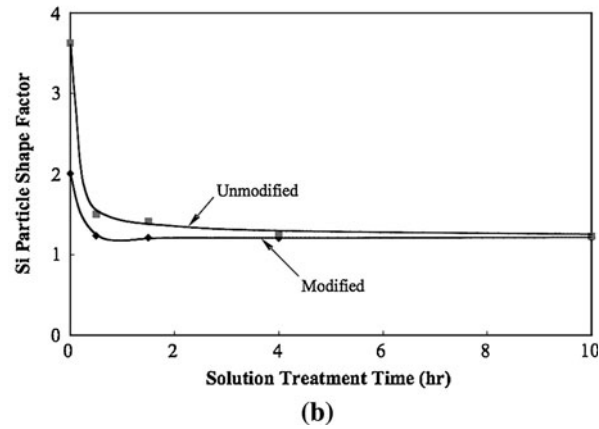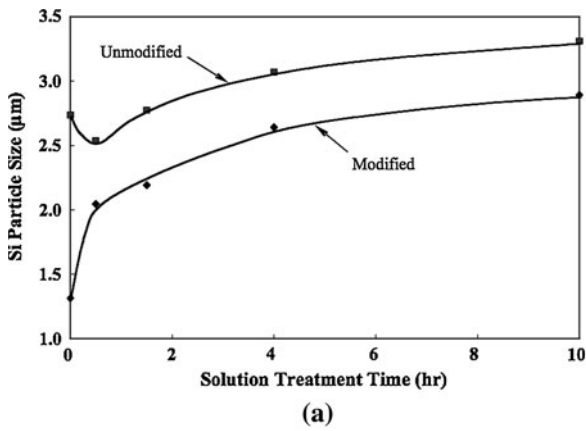
(a)

(b)

Fig. 4—The effects of solution treatment time on (*a*) the size and (*b*) the shape factor of the eutectic Si particles. Shape factor = perimeter^2/(4 × π × area).

Fig. 5—UTS of the five alloys evaluated after a T61 heat treatment carried out at different solution treatment times (0 h represents the as-cast condition).

Fig. 6—YS of the five alloys evaluated after a T61 heat treatment carried out at different solution treatment times (0 h represents the as-cast condition).
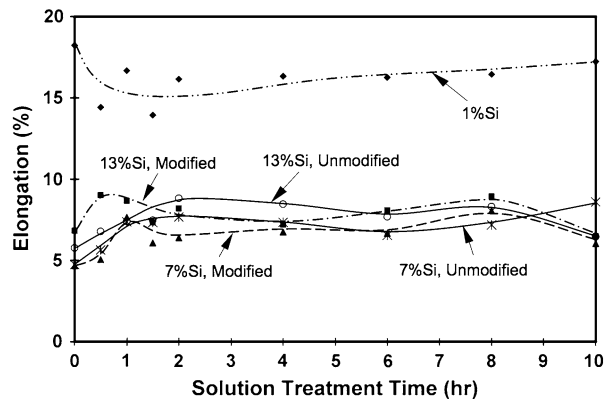
Fig. 7—Elongation of the five alloys evaluated after a T61 heat treatment carried out at different solution treatment times (0 h represents the as-cast condition).

and with a slower rate after 0.5 hours. It should be noted that the fast growth observed at the beginning is from data, which is evaluated from 2D images, that do not represent the 3D complexities of the particles, especially for as-cast modified particles. The as-cast modified Si particles are fibrous and branched in 3D (Figure 3, left), but they appear as small and round particles in 2D images (Figure 2, left). Under these circumstances, the measured particle size for the modified alloys is much smaller than the actual value. In fact, at the beginning of the solution treatment, the fibrous particles fragment and their size decreases just as in the case of unmodified alloys (Figure 3).

B. *Mechanical Properties*

Figures 5, 6, and 7 present the variation of UTS, YS, and e pct with solution treatment time for all alloys evaluated. The 0-hour solution treatment time represents the as-cast conditions, and the rest of the data originate from specimens solution treated for different times, naturally aged, and then artificially aged for 12 hours (T61). Selected values of UTS, YS, and e pct for all alloys in as-cast conditions, T61 (solution treated at 811 K [538 °C] for 10 hours, quenched, natura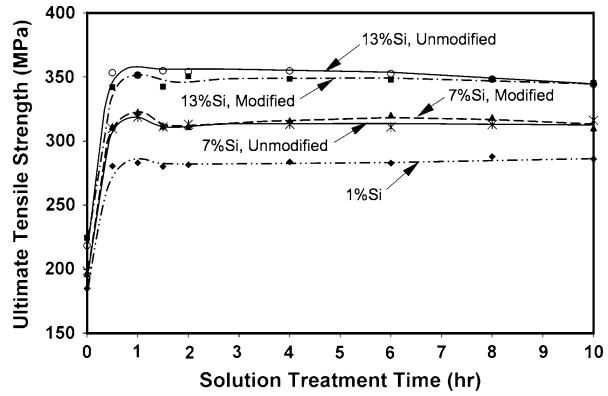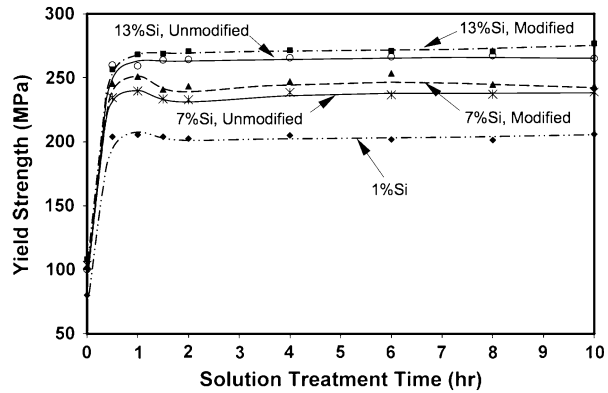lly aged, and artificially aged at 428 K [155 °C] for 12 hours), and T4 (solution treated at 811 K [538 °C] for 10 hours and quenched without aging, which is not shown in the figures), are tabulated in Table II.

As observed in Figures 5 and 6, the UTS and YS of all five alloys increase significantly after heat treatment compared with the as-cast condition, with most of the increase occurring in the first 0.5 hours of solution treatment. The peak values are reached somewhere between 0.5 and 1.5 hours. Passing the peaks, both UTS and YS decrease, reaching minimum values around 1.5 hours. The amounts of decrease from the peaks are different for different alloys; the alloys with 7 pct Si have the largest decrease. After ~1.5 hours, the UTS and YS show generally a slight increase, reaching values close to the peaks at solution treatment times between 6 to 10 hours (except for the unmodified 13 pct Si alloy, which shows a slight decrease in UTS).

The variations in e pct are slightly different from those of UTS and YS. For the modified alloys, both 7 and 13 pct Si alloys, the e pct increases significantly at the beginning of the solution treatment, reaches a peak between 0.5 and 1.5 hours, decreases to a minimum point between 1.5 and 2 hours, increases again to a second peak between 7 and 9 hours, and finally, decreases again to values close to the as-cast values. For the unmodified alloys, the same trends are observed but the transitions happen at a slower rate. For the unmodified 7 and 13 pct Si alloys, the e pct reaches the first peak between 1.5 to 2.5 hours, decreases to a lower point between 5 and 7 hours, and reaches the second peak between 8 and 10 hours. For both 7 and 13 pct Si alloys, in modified as well as unmodified conditions, the second peaks are equal to or slightly higher than their respective first peaks. The e pct of the 1 pct Si alloy decreases significantly at the onset, up to ~2 hours; then elongation slowly increases, reaching a value close to that of the as-cast condition at ~10 hours.

C. Effect of Si Content and Morphology on UTS and YS

For all five alloys studied, UTS and YS increase with increasing Si content in both as-cast and T61 heat-treating conditions for all solution treatment times. For example, in the as-cast condition, the YS of alloys 1 (1 pct Si), 2, and 4 (unmodified 7 and 13 pct Si) are 80 MPa (11.6 ksi), 103 MPa (15 ksi), and 100 MPa (14.5 ksi), respectively. The YS of these alloys after T61 heat treatment are 203 MPa (29.5 ksi), 238 MPa (34.5 ksi), and 266 MPa (38.6 ksi)—averaged from solution treatment times of 4, 6, 8, and 10 hours. The data were fitted with the following exponential equation, which can be used to estimate the effect of Si content on YS for T61-treated Al-Si-0.45 pct Mg alloys with Si content in the 1 to 13 pct range:

$$YS(MPa) = 203 + 7.63 \times (pct\,Si - 1)^{0.85}$$

or

$$YS(ksi) = 29.44 + 1.11 \times (pct\,Si - 1)^{0.85}$$

The Si content has a similar effect on UTS, and the equation can be written as follows:

$$UTS(MPa) = 286 + 3.56 \times (pct\,Si - 1)^{1.13}$$

or

$$UTS(ksi) = 41.48 + 0.52 \times (pct\,Si - 1)^{1.13}$$

Sr modification increases the YS of 7 and 13 pct Si alloys in all T61 conditions, but it shows little influence on the UTS. The modified 7 pct Si alloy (alloy 3) has a slightly higher UTS than the unmodified 7 pct Si alloy (alloy 2) after T61 with a solution treatment time of 6 hours; at prolonged solution treatment times, the UTS of alloys 3 and 2 become similar (Figure 5). Modification does not show much influence on the UTS of 13 pct Si alloys after a T61 treatment.

For all alloys, the e pct increases significantly at T4, and it decreases after aging (T61). The e pct decreases significantly with increasing Si from 1 to 7 pct for all solutionizing conditions. When Si is increased from 7 to 13 pct, the e pct is not greatly affected, and the unmodified and modified alloys alternatively go through conditions of maxima and minima. However, as mentioned earlier, the e pct varies differently with solution treatment time for modified and unmodified alloys.

It is shown that the responsiveness (i.e., the property variation rate) of the alloy to heat treatment is influenced by the Si content. After heat treatment, the alloys with a higher Si content experience larger increases in both UTS and YS; the higher the Si content, the greater the change in UTS and YS. For example, for the 7 pct Si alloy, the increase in YS from as-cast to T61 heat-treating conditions is 138 MPa (20.1 ksi), whereas for the 13 pct Si alloy, it is 167 MPa (24.2 ksi); values were calculated from the average of unmodified and modified alloys for both 7 pct (alloys 2 and 3) and 13 pct Si (alloys 4 and 5) alloys. A similar response is observed for the UTS when comparing as-cast and T61 conditions.

V. DISCUSSION

A. Effects of Solution Treatment Time

In the T61 treatment, most changes in mechanical properties take place at short solution treatment time (less than 1 hour). More than 95 pct of the increase in UTS and YS (and even their maximum values) can be achieved with solution treatments of around 1 hour or less. The variations in e pct with solution treatment time are larger than those in UTS and YS, and the largest variations occur at solution treatment times (1 to 1.5 hours). The reasons behind these observations are attributed to various factors.

The alloy strengthening is mainly a result of the formation of Mg-Si precipitates from dissolved Si and Mg. The dissolved Si and Mg originate from the dissolution of as-cast Mg_2Si precipitates and Si particles. The dissolution leaves vacancies and creates distortions in the Al matrix crystals. As discussed earlier, the dissolution of Si and Mg is complete at short solution treatment times[4] and leaves large amounts of vacancies and distortions. In a short time, the atoms will not have enough time to rearrange to fill and correct these vacancies and distortions, and these vacancies and

Table II. Tensile Properties of the Tested Alloys in As-Cast, T4, and T61 Conditions

Alloy	UTS – MPa (ksi)			YS – Mpa (ksi)			e pct		
	As-Cast	T4*	T61**	As-Cast	T4	T61	As-Cast	T4	T61
Alloy 1 (1 pct Si)	185 (26.8)	245 (35.5)	286 (41.5)	80 (11.6)	126 (18.3)	206 (29.9)	18.2	28.5	17.2
Alloy 2 (7 pct Si unmodified)	199 (28.8)	262 (38.0)	316 (45.9)	103 (15.0)	137 (19.8)	239 (34.7)	4.7	12.5	6.0
Alloy 3 (7 pct Si Sr-modified)	197 (28.5)	265 (38.5)	310 (45.0)	103 (14.9)	141 (20.4)	243 (35.3)	4.7	15.5	6.5
Alloy 4 (13 pct Si unmodified)	219 (31.7)	296 (43.0)	344 (49.9)	100 (14.5)	162 (23.5)	265 (38.5)	5.8	11.5	8.6
Alloy 5 (13 pct Si Sr-modified)	225 (32.6)	286 (41.5)	345 (50.1)	108 (15.7)	159 (23.1)	277 (40.2)	6.8	10.0	6.5

*T4 solutionized at 811 K (538 °C) for 10 hours and quenched without artificial aging.
**T61 solutionized at 811 K (538 °C) for 10 hours, quenched, naturally aged, and artificially aged at 428 K (155 °C) for 12 hours.

distortions act as nuclei and facilitate the formation of large amount of fine Mg-Si particle precipitates and thus strengthen the alloy.

The eutectic Si particles also strengthen the alloy. For the same amount of Si, smaller and more uniformly distributed particles have a stronger effect. The fragmentation of Si particles reduces the particle size and increases the particle number and thus strengthens the alloy. The fragmentation of the eutectic Si takes place mostly at the early stage of solution treatment (Figures 2 and 3), and so, the strengthening effect caused by the morphology variation of Si particles occurs mostly in this time.

Most strengthening effects from Mg-Si precipitation, crystal distortion, and Si particle fragmentation occur at short solution treatment time, and thus, the alloy's strength increases rapidly during this period. Because the dissolution of Mg and Si is complete at short solution treatment time, a longer solution treatment does not add more vacancies and/or distortions. Instead, the earlier formed vacancies and distortions are reduced and smoothened and become less and less active as nuclei, resulting in fewer Mg-Si precipitates and slowing the increase in strength. The reduction in vacancies and distortion itself also reduces the strengthening effect. As a result, the strength reaches a peak and then slightly decreases. The time when the reduction in strength stops corresponds to the time when all vacancies are filled and the distortion is recovered. Thereafter (*i.e.*, after ~1.5 hours), the strength variation mainly will be determined by changes in Si particle size and morphology. Si fragmentation still may be occurring, but slowly, and at the same time, Si particles are spheroidized and coarsened. In this time, the strengthening effect caused by Si fragmentation is counteracted by the weakening effects of coarsening and spheroidization, resulting in small variations in strength.

Elongation is affected by many factors, including eutectic Si, as-cast and precipitated Mg-Si, casting defects (such as porosity and inclusions), segregation, residual stress, *etc*. Generally, solution treatment homogenizes the microstructure by dissolving the as-cast Mg_2Si precipitates as well as some inclusions and intermetallics (such as Cu-rich compounds in Al), it reduces segregation, and spheroidizes pores, intermetallics, and inclusions, which all improve e pct. However, subsequent quenching creates residual stresses and

reduces e pct. During aging, the formation of Mg-Si precipitates reduces the e pct, whereas the release in residual stress improves it. The data in Table II show that, for all studied alloys, the homogenization (increasing the elongation) and precipitation of Mg-Si (reducing the elongation) play more important roles than the relief in residual stress (increasing the elongation), which is why a significant decrease in elongation is observed after aging subsequent to the initial increase corresponding to T4.

B. *Effects of Si Content*

For all testing conditions, the alloys with a higher Si content have higher UTS and YS than those with a lower Si content. The variation in strength with Si content only can be attributed to the amount of eutectic Si. Si particles strengthen the alloys, and a higher Si content creates more eutectic Si particles and produces a greater strengthening effect.

Because the Al matrix is saturated with Mg and Si after a short solution treatment, the Al matrices of all evaluated alloys should be the same when the alloys are solution treated for a longer time (>1.5 hours). If the alloy properties only were influenced by Mg-Si precipitation, then the changes in the properties of the alloys after T61 should be proportional to the volume fraction of the Al matrix. In other words, the 1 pct Si alloy should experience the largest property change after T61 because it consists of only the Al matrix with dissolved Mg and Si after T4, followed by 7 and 13 pct Si alloys, which contain eutectic structures and therefore less amounts of Al matrix. However, the UTS and YS results after T61 show that the alloys with a higher Si have experienced greater changes than the 1 pct Si alloy. For example, the increases in YS from the as-cast condition are 126 MPa (18.3 ksi) for the 1 pct Si alloy, ~140 MPa (20.4 ksi) for the 7 pct Si alloy, and ~169 MPa (24.5 ksi) for the 13 pct Si alloy (Table II, modified alloys). These results indicate that the Si content influences the alloy's response to heat treatment, and the higher the Si content, the stronger the response of the UTS and YS. This effect is attributed to the evolution in size and morphology of the eutectic Si particles as a result of heat treatment because the eutectic structure is the only differing variable among the alloys. The factor, which makes the higher Si alloys

have a stronger response in UTS and YS during heat treatment, is mainly the fragmentation of Si particles. The fragmentation of Si particles strengthens the alloys, and thus, in the alloys with a higher Si content, the fragmentation produces more small particles, which induces higher strengthening effects.

Generally, the alloys with a higher Si content have lower e pct because the Si particles at the interphase boundaries increase the resistance to dislocation movement, which strengthens the alloy and reduces its ductility. For example, the e pct of 7 pct Si alloys (alloys 2 and 3) is much lower than that of the 1 pct Si alloy (alloy 1). However, when the Si level was increased to 13 pct, the e pct did not decrease any more, and in fact, it increased for as-cast conditions. The increase in ductility with Si content also has been reported for other casting Al alloys such as Al-Si-Cu-Mg alloys.[17] This finding was explained by the fact that increased Si has a size-refining effect on the intermetallics formed from the eutectic liquid, and the increase in Si distributes the intermetallics more uniformly within the interdendritic and intergranular regions. Another reason can be related to porosity because the 13 pct Si alloys have lower shrinkage and less total and interdendritic porosity than the 7 pct Si alloys.

Residual stress also may reduce e pct. Alloys with different Si contents can result in different residual stress levels during the same process. The alloy with low Si (e.g., 1 pct Si) consists basically of Al; it is ductile, it has lower YS, and thus, the residual stress level produced after T4 treatment should be low. The alloys with higher Si (e.g., 7 and 13 pct Si) have large amounts of eutectic Si particles and thus higher YS (lower e pct) and higher residual stress levels after T4. Thus, in these alloys, in the T4 condition, increasing residual stress will decrease the e pct, which counteracts the increase in e pct caused by homogenization. During aging, the release of residual stress in the alloy with higher Si can improve the e pct, which counteracts the e pct reduction caused by Mg-Si precipitation. As a result, the alloys with a higher Si content have smaller variations in e pct. This explains why, in as-cast conditions, the alloys with a higher Si have a higher residual stress and thus a lower e pct and why their e pct improves after T61, whereas the e pct of the 1 pct Si alloy decreases (Figure 7).

C. *Optimum Solution Treatment Time*

In the T61 conditions, the UTS, YS, and e pct of the alloys studied reach their peak values at short solution treatment times (0.5 to 1.5 hours range), and these peak values are the maximum or the near maximum values that can be reached. This finding suggests that for improving UTS, YS, and e pct, a long heat treatment time may not be needed. However, when selecting the heat treatment time, various factors need to be considered. Peak values are reached at different solution treatment times for different properties and different alloys; moreover, around the peak, the properties vary significantly. The solution time at which the peak is reached is affected by several factors, such as Si content,

size and morphology, SDAS, casting size and geometry, casting wall thickness, heating method, and the arrangements of the castings in the furnace. All these factors need to be assessed when shortening the solution treatment time below 4 hours.

VI. CONCLUSIONS

The morphology of the eutectic Si particles changes significantly with solution treatment time; it undergoes the following transformations: fragmentation, spheroidization, and growth. Most fragmentation occurred in less than 0.5 hours for the modified alloys, whereas the fragmentation continued longer than 4 hours (even though the most significant transformations occurred within 1.5 hours) for the unmodified alloys. In the modified alloys, the Si particles became rounder and started to grow in less than 0.5 hours, whereas in the unmodified alloys, no significant growth was observed even after 10 hours of solution treatment. The dominant phenomenon at any given time depends on the treatment temperature and the size and morphology of the original particles.

In the T61 treatment, most changes in mechanical properties take place at short solution treatment times (less than 1 hour). More than 95 pct of the increase in UTS and YS (and even their maximum values) can be achieved with solution treatments of ~1 hour or less because most strengthening effects from Mg-Si precipitation, crystal distortion, and Si particle fragmentation occur at short solution treatment times. The formation of Mg-Si precipitates from dissolved Si and Mg is the main alloy-strengthening factor. The dissolution of Si and Mg is complete at short solution treatment times and leaves large amounts of vacancies and distortions. These vacancies and distortions will not be filled and recovered in short times; they act as nuclei that facilitate the formation of a large amount of fine Mg-Si precipitates. The variations in e pct with solution treatment time are larger than those in UTS and YS, but the largest variations occur at short solution treatment times (1 to 1.5 hours).

For all the studied alloys, UTS and YS increase with an increasing Si content in both as-cast and T61 heat-treating conditions for all solution treatment times. The e pct increases significantly after solution treatment (T4) and decreases after artificial aging (T61). The e pct decreases significantly with an increasing Si level from 1 pct to 7 pct for all solutionizing conditions. When Si is increased from 7 pct to 13 pct, the e pct is not much affected.

The Si content also affects alloys' response to heat treatment. After T61, the alloys with a higher Si content experience larger increases in both UTS and YS; the higher the Si content, the greater the change in UTS and YS. This effect can be attributed to fragmentation of Si particles. Fragmentation of Si particles strengthens the alloys, and in the alloys with a higher Si content, the fragmentation produces more small particles and induces higher strengthening effects.

Improvements in UTS, YS, and e pct can be achieved at short solution treatment times; however, when selecting the heat treatment time, various factors need to be considered judiciously.

REFERENCES

1. *ASM Handbook, Heat Treatment*, vol. 4, ASM, Materials Park, OH, 1991, pp. 849–50.
2. J.R. Davis: *Aluminum and Aluminum Alloys*, ASM, Materials Park, OH, 1993, pp. 297–98.
3. B. Closset, R.A.L. Drew, and J.E. Gruzleski: *AFS Trans.*, 1986, vol. 94, pp. 9–16.
4. D. Apelian, S. Shivkumar, and G. Sigworth: *AFS Trans.*, 1989, vol. 97, pp. 727–42.
5. H.J. Li, S. Shivkumar, X.J. Luo, and D. Apelian: *Cast Metals*, 1989, vol. 1 (4), pp. 227–34.
6. B.A. Parker, D.S. Saunder, and J.R. Griffiths: *Met. Forum*, 1982, vol. 5 (1), pp. 48–53.
7. E.N. Pan, J.F. Hu, and C.C. Fan: *AFS Trans.*, 1996, vol. 104, pp. 1119–32.
8. L. Pedersen and L. Arnberg: *Metall. Mater. Trans. A*, 2001, vol. 32A, pp. 525–32.
9. C.W. Meyers: *AFS Trans.*, 1985, vol. 93, pp. 741–50.
10. S. Shivkumar, S. Ricci, Jr., and D. Apelian: *AFS Trans*, 1990, vol. 98, pp. 913–22.
11. R. Li: *AFS Trans.*, 1996, vol. 104, pp. 777–83.
12. C.W. Meyers: *AFS Trans.*, 1986, vol. 94, pp. 511–18.
13. M. Kaczorowski: *Aluminum*, 1984, vol. 60, pp. 177–79.
14. J.P. Lynch, M. Brown, and H. Jacobs: *Acta Metall.*, 1982, vol. 30, pp. 1389–94.
15. K.T. Kashyap, S. Murali, K.S. Raman, and K.S. Murthy: *Mater. Sci. Technol.*, 1993, vol. 9, pp. 189–203.
16. Y. Langsrud and S. Brusethanug: *Aluminum*, 1999, vol. 75, pp. 980–87.
17. C.H. Caceres and J.A. Taylor: *Proc. of TMS 2005, 134th Annual Meeting and Exhibition*, San Francisco, CA, 2005, pp. 245–54.